Optimization of pretreatment in pymetrozine production wastewater via reactive distillation and side-stream distillation methods with response surface methodology

Qi Chen, Kaijun Wang, Qixing Cai, Zhenggui Gu and Jianzhong Zhu

ABSTRACT

Lots of highly concentrated saline organic wastewater is produced during the pymetrozine production process, causing environmental pollution and waste of resources if discharged directly. Research on actual pymetrozine wastewater treatment is quite scarce. Existing treatment methods of pesticide wastewater usually have disadvantages of long treatment time, low processing efficiency and low recovery rate. To solve these problems, a pretreatment process for pymetrozine wastewater was studied based on material recovery and pollutant degradation. The ammonia conversion process was experimentally investigated by reactive distillation. The reaction product vapor was neutralized and then separated by side-stream distillation. Aspen Plus and response surface methodology were employed to simulate and optimize the operating conditions. Box-Behnken design was used to investigate the individual and interaction effects on methanol purification and sodium acetate removal. Experimental study was carried out on the basis of theoretical simulation data. The result showed that the optimized methanol content on tower top was 99.28% with a yield of 99.95% and methanol content of side withdrawal was 0.01%. The process can be applied for pesticide wastewater treatment to recycle high purity chemical materials, and meets the national sewage comprehensive emission standard.

Key words | Aspen Plus, Box-Behnken design, pymetrozine production wastewater, reactive distillation, response surface methodology, side-stream distillation

HIGHLIGHTS

- Pretreatment process of pymetrozine production wastewater is presented.
- Reactive distillation is carried out for ammonia conversion treatment.
- Side-stream distillation is operated for methanol and ammonium sulfate recycling, using Aspen Plus and RSM as the simulation and optimization tools.
- The process helps in recycling methanol of 99.28 wt.% and reaching wastewater discharge standard.

Qi Chen
Jianzhong Zhu (corresponding author)
Key Laboratory of Integrated Regulation and Resource Development on Shallow Lake of Ministry of Education, College of Environment,
Hohai University,
Nanjing 210098,
China
E-mail: *zhuhhai2010@hhu.edu.cn*

Qi Chen
School of Biology and Environment,
Nanjing Polytechnic Institute,
Nanjing 210048,
China

Kaijun Wang
Qixing Cai
Zhenggui Gu
Jiangsu Provincial Key Laboratory of Materials Cycling and Pollution Control,
Nanjing Normal University,
Nanjing 210023,
China

doi: 10.2166/wst.2020.599

GRAPHICAL ABSTRACT

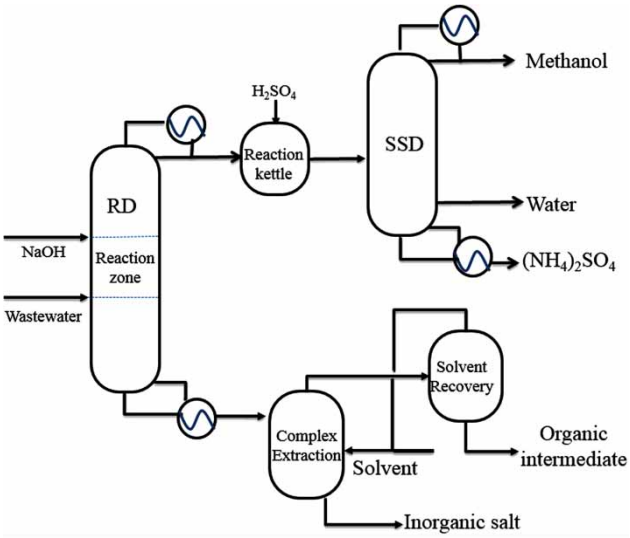

INTRODUCTION

Pymetrozine is a systemic pesticide of the pyridine-azomethin family (Khan *et al.* 2018). It is used as insecticide to control whiteflies, leafhoppers and cotton aphids in crops, due to its high activity and superior insecticidal effect (Fdez-Sanromán *et al.* 2020). Because of its extensive use, improper disposal, accumulation ability, long persistence in the environment and long-term effect on living organisms, pymetrozine has been classified as a "likely" human carcinogen and registered for crops with maximum residue in some countries (Jang *et al.* 2014).

The traditional process of synthesizing pymetrozine is complicated. Multi-step processes are included such as hydrazinolysis, cyclization, alkylation, condensation, hydrolysis (Wang *et al.* 2012). The synthesis of pymetrozine was conducted as shown in Figure 1 (Zhou *et al.* 2018). Acetohydrazide (Intermediate I) was obtained via hydrazinolysis using ethyl acetate and hydrazine hydrate as starting materials and then cyclized with phosgene to give Intermediate II. After reaction with chloroacetone, ring-opening reaction and cyclization gave Intermediate III. Then Intermediate III was treated with hydrazine hydrate to obtain Intermediate IV. Subsequently, hydrolysis in the presence of hydrochloric acid and methanol (CH_4O) is carried out to afford Intermediate V. The desired product, pymetrozine, is obtained via the condensation of nicotinaldehyde with Intermediate V in the presence of sodium hydrate.

As stated above, a large amount of wastewater was produced, including but not limited to CH_4O, salty substance (ammonium acetate and sodium acetate), water (H_2O) and a large amount of intermediates of pesticides. As a kind of poor degradable organic wastewater, pymetrozine production wastewater is characterized by high chemical oxygen demand, acidity and high biotoxicity. Most of all, nitrogenous organic compounds in pesticide intermediates will cause microbial toxicity and have a great impact on subsequent biological treatment.

At present, studies on pymetrozine mainly focus on the analysis method (Hou *et al.* 2019), properties (Olfati Somar *et al.* 2019), degradations and potential health risk in ecosystems (Elfikrie *et al.* 2020). But research on actual pymetrozine production wastewater treatment is quite scarce.

Conventional wastewater treatment technologies focus on nutrient and pathogen removal, and are generally ineffective in pesticide removal (Sutton *et al.* 2019). The treatment methods for pesticide wastewater mainly include physical methods, chemistry methods, biochemical methods and comprehensive methods. Physical methods are used as pretreatment methods for recovering by-products and mainly include extraction (De Gaetano *et al.* 2016), adsorption (Rajapaksha *et al.* 2018) and membrane separation (Qin *et al.* 2020). But a single physical method doesn't work well due to the strong polarity and water solubility of the organic

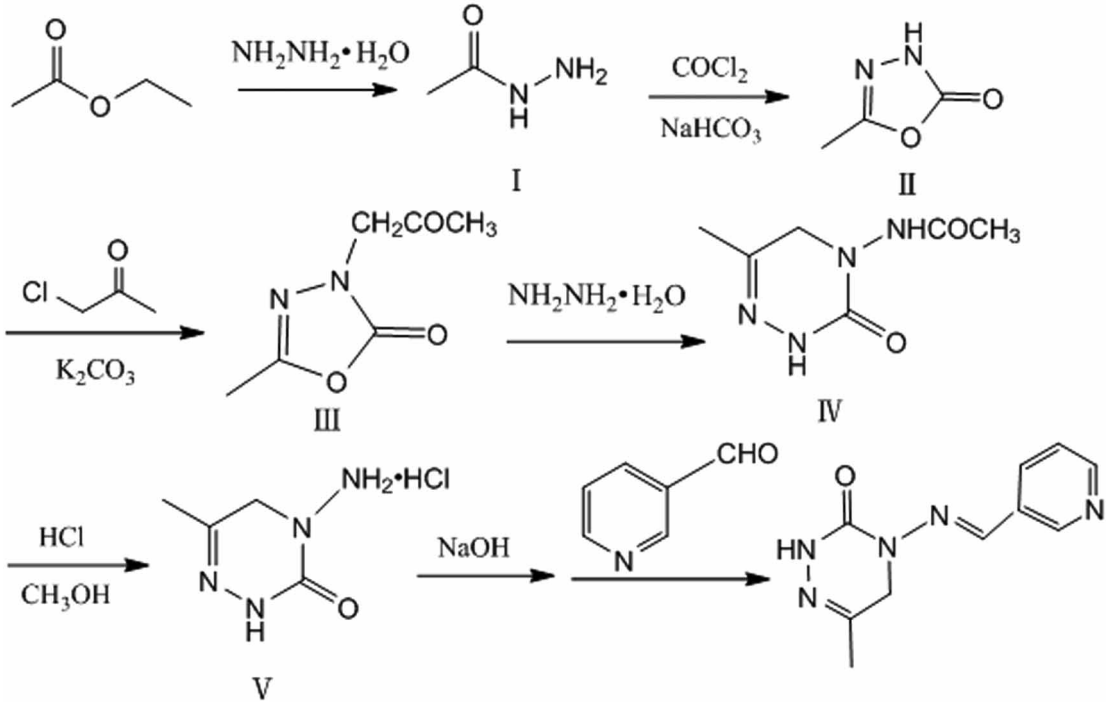

Figure 1 | Traditional synthetic route for pymetrozine.

substances in pesticide wastewater. Chemistry methods, as pretreatment processes for biochemical treatment to improve the biodegradability, mainly consist of chemical oxidation (Carra *et al.* 2016), electro catalytic oxidation microwave assisted catalysts (Tony & Mansour 2019), and so on. The disadvantage of chemistry methods is that compounds are degraded and cannot be reused, in spite of the high degradation rate. Biochemical methods, used as the main treatment process after pretreatment, have disadvantages of long treatment time and low efficiency. Comprehensive methods such as bio-Fenton and bio-electro-Fenton (Kahoush *et al.* 2018), need to improve the performance, stability and lifetime to achieve more sustainable and cost-effective wastewater treatment. Combined with the research above, sufficient attention should be paid to the pretreatment of pymetrozine production wastewater, which may have a detrimental effect on the environment.

For the purpose of solving practical problems, the pretreatment process for pymetrozine production wastewater was investigated in this paper. The research technical route is shown in Figure 2. The wastewater was initially placed in a reactive distillation apparatus for ammonia conversion treatment, taking advantage of the poor stability of ammonium acetate (NH_4AC). By adding NaOH, NH_4AC was converted into NaAC and free ammonia. Reactive distillation (RD) was chosen due to its specific advantages, such as improved selectivity, increased conversion, effective utilization of reaction heat, reduced capital investment, and so on. With the combination of reaction and separation, RD can shift the equilibrium of reaction towards the product side by continuous removal of the products and give higher conversions (Gor *et al.* 2020).

Free ammonia and CH_4O collected from the top of RD were neutralized and then separated by side-stream distillation (SSD) and NaAC in the mixed salt could be purified. Due to the high energy-efficiency and easy operation, SSD is preferred instead of conventional distillation (Tututi-Avila *et al.* 2017). The Aspen Plus system was used to simulate the SSD process, with Radfrac as the rectification module. Box-Behnken design (BBD), based on response surface methodology (RSM), was applied for experimental design of the SSD process to investigate the effects of different operating conditions on methanol removal and ammonium sulfate ($(NH_4)_2SO_4$) purification.

The residue collected from the bottom of the RD unit contains a large amount of organic nitrogen components such as pymetrozine, 3-aminopyridine, and 4-Acetylamino-6-methyl-3-oxo-2,3,4,5-tetrahydro-1,2,4-triazine, and so on. The purification of organic nitrogen components has been researched by our research team in another article (Wang *et al.* 2020), by complex extraction process with p204 (di (2-ethylhexyl) phosphate) as the complexing agent and benzene as the diluent agent.

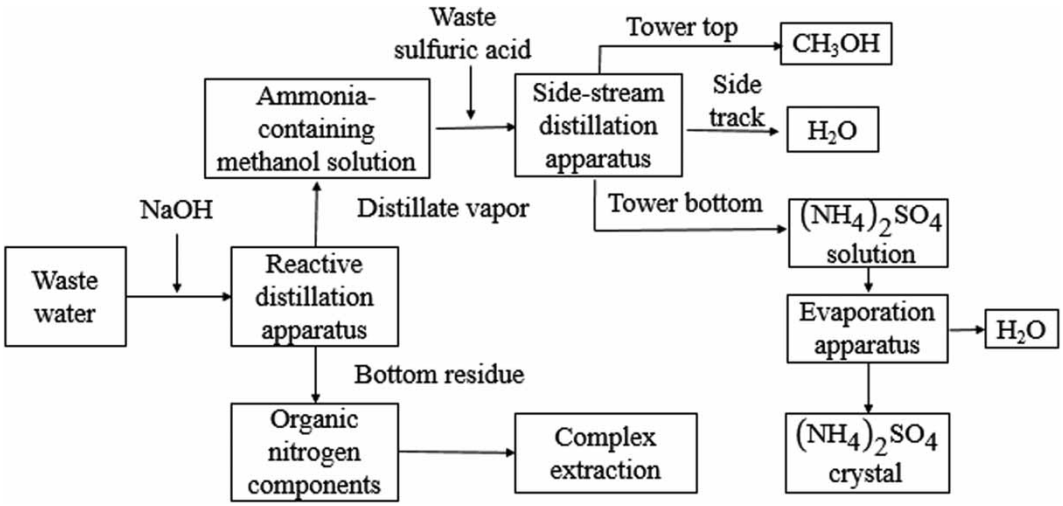

Figure 2 | The research technical route.

A complete set of recovery and treatment technology for pymetrozine production wastewater is proposed in this paper. The main purpose is to assess pretreatment process of pymetrozine production wastewater by reactive distillation and side-stream distillation methods using Aspen Plus as the simulation tool and RSM as the optimization tool. The chemical materials with high purity and high added value can be separated effectively, including ammonia, CH_4O, nitrogenous organic compounds and inorganic salts. Moreover, the treated wastewater, with low chemical oxygen demand (COD) content and greatly reduced toxicity, can be directly discharged into a biochemical treatment plant, and then reach the 'national sewage comprehensive emission standard' (GB8978-1996). Therefore, it can obtain high economic benefits and good wastewater treatment effect.

MATERIALS AND METHODS

Materials

All the reagents were analytical grade and used directly without any further purification. Sodium hydroxide (NaOH) and sulfuric acid (H_2SO_4) were purchased from Sinopharm Chemical Reagent Co.Ltd (China) with purity of 99.5%. Pymetrozine production wastewater was collected from a waste liquid discharge port of a pesticide-producing enterprise located in Yancheng City, Jiangsu Province. Main physical properties of pymetrozine wastewater used in this research are shown in Table 1.

Methods

Experiment procedure of ammonia conversion treatment

Experimental procedure was designed as shown in Figure 3. 300 mL of pymetrozine production wastewater and 100 mL of NaOH solution were poured into a three-necked flask through a constant pressure dropping funnel. The condensate water, magnetic stirrer, pH meter and heating jacket were kept working continuously. The distillate vapor was condensed through the spherical condensing tube, and collected in the oil-water separator. The condensed fluid was taken out for CH_4O analysis. pH variation was detected every 10 minutes by pH meter with a certain accuracy (0.01). When no more CH_4O was detected in the liquid from the oil-water separator, it was considered that CH_4O had been steamed out completely, and the reaction was terminated. The remaining liquid in the three-bottle flask was

Table 1 | Physical properties of pymetrozine wastewater and neutralized distillate

Material	pH	Composition of CH_4O (wt.%)	Composition of H_2O (wt.%)	Composition of $(NH_4)_2SO_4$ (wt.%)	Composition of salinity (wt.%)	Composition of pesticide intermediates (wt.%)
Raw material	5.73	9.43	77.69	_	10.23	2.65
Neutralized distillate	7.82	14.90	78.96	6.14	_	_

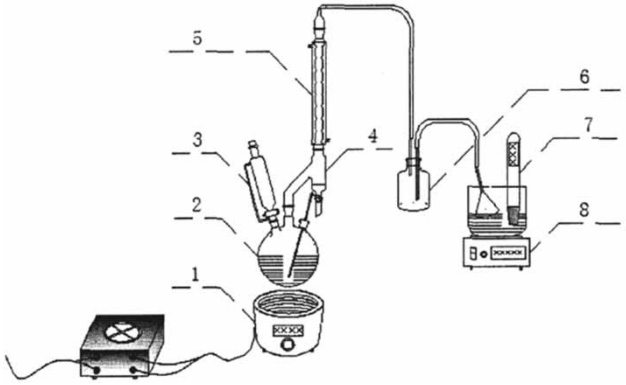

Figure 3 | Reactive distillation apparatus. 1. heating jacket 2. three-necked flask 3. dropping funnel 4. oil-water separator. 5. spherical condenser tube 6. surge flask 7. pH meter 8. magnetic stirrers.

weighed, and a small amount of liquid was taken for elemental analysis. H_2SO_4 was selected to neutralize the distillate vapor of ammonia (NH_3) into $(NH_4)_2SO_4$ in surge flask.

Elemental analysis method

Vario EL elemental analyzer (Germany Elementar Company) was used for elemental analysis, with JY/T017-1996 elemental analyzer general rules as the analysis detection principle. The quality content of nitrogen element (ω_N) was measured as 2.49%. The mass fractions of NH_4AC (ω_{NH_4AC}) and the theoretical amount of NaOH (m_{NaOH}) required for neutralization reaction were calculated by the following equations, on the premise of NH_4AC as the only nitrogen taking part in the reaction:

$$\omega_{NH_4AC} = \frac{\omega_N \times 77.08}{14} \times 100\% = 13.71\% \quad (1)$$

$$m_{NaOH} = \frac{100 \times \omega_{NH_4AC}}{77.08} \times 40 = 7.12\ g \quad (2)$$

where ω_N, Mr_{NH_4AC}, Ar_N, Mr_{NaOH} and 100 are respectively, the quality content of nitrogen element, the relative molecular mass of NH_4AC, the relative atomic mass of nitrogen element, the relative molecular mass of NaOH and 100 g of waste liquid. Thus, the theoretical addition amount of NaOH was calculated as 7.12 g per l00 g of waste liquid. Since almost all organic pesticides contain nitrogen element, ω_{NH_4AC} determined by this method was only a reference.

Thermal conductivity detection

SP-6800 Gas chromatography (Luann Chemical Instrument Factory) was used for thermal conductivity detection, with a chromatographic column of 4*100 mm stainless steel tube, white GDX-102 supports, stationary liquid isophthalic acid, thermal conductivity cell detector, nitrogen carrier gas, and a column pressure of 0.1 MPa. The operating conditions were 120 °C in the gasification chamber, 80 °C in the column, 130 °C in the detector, and the sample injection quantity was 2 μL. When the temperature of the vaporizer was 120 °C, only CH_4O and H_2O were detected and the composition of CH_4O was 10.82 wt.%. It was preliminarily determined that the boiling points of pesticide intermediates and salty substances contained in the wastewater were basically higher than 120 °C, and the removing process of free ammonia and CH_4O by reaction distillation had no effect on high boiling point material. The composition of CH_4O in pymetrozine wastewater was 9.43 wt. % by comprehensive calculation.

The product collected from the top of RD was neutralized and detected by gas thermal conductance. The mass fractions of CH_4O and H_2O were 15.87% and 84.13% respectively. The quality percentage of $(NH_4)_2SO_4$ was calculated to be 6.14% by evaporation crystallization technology. In conclusion, the integrated composition of the neutralized distillate was calculated as follows: the mass percentages of CH_4O, $(NH_4)_2SO_4$ and H_2O were 14.90%, 6.14% and 78.96% respectively. The main physical properties of neutralized distillate are shown in Table 1.

SSD simulation procedure by Aspen Plus

The product collected from the top of RD was separated by SSD for recycling a high concentration of methanol on the tower top and $(NH_4)_2SO_4$ from the tower bottom, aiming at methanol content on the tower top (ω_{CH_4O-1}) of more than 99% and methanol content of side withdrawal (ω_{CH_4O-2}) of less than 0.1%. Single factor experiments were designed based on Aspen Plus to investigate the effect of operating conditions on SSD, which provided the data foundation for the next BBD experimental design and RSM.

As the separation system was a polar and electrolytic system, the ELECNRTL property method and Radfrac rectification module were selected for SSD simulation by Aspen Plus. The influence of operating conditions was investigated, and the proper range of the main factors were preliminarily determined, such as number of stages (N), reflux ratio (R), feeding stage (N_F), side line outlet stage (N_S), distillate rate (D_1) and sideline discharge rate (D_2), as shown in Table 2.

Table 2 | Parameters of experiment simulation

Parameter	Value	Parameter	Value	Parameter	Value
F/(Kg/h)	100	T_F/°C	20.0	Property method	ELECNRTL
D_1	0.11 ~ 0.18	T_D/°C	65.0	N	15 ~ 28
D_2	0.30 ~ 0.75	T_W/°C	102.1	N_F	3 ~ 15
R	1 ~ 7	T_S/°C	99.9	N_S	13 ~ 24
Feedstock	$(NH_4)_2SO_4$-CH_4O-H_2O				

Statistical analysis by BBD-RSM

The evaluation of the experimental design was performed using Design-Experts® version 10 software. RSM is an experimental and analytical software, with a whole set of mathematical and statistical models to optimize operating conditions for a multivariable system (Wei *et al.* 2020). BBD, one of the main types of RSM, is a less time-consuming approach that allows evaluation of all possible parameter interactions (Karthikeyan *et al.* 2010), and uses fewer design points, with fewer experiments to run, compared with central composite designs (CCD), another main types of RSM. It represents advantages of time and materials consumed and economics of process development (Cordova-Villegas *et al.* 2019). Four independent variables were selected; that is, N, N_F, D_1 and R, with ω_{CH_4O} as the response (dependent variable), and interactions between variables and the response were obtained. In order to optimize BBD, a three-level-four-factor design was applied, and 29 runs were generated. The actual and coded levels of the variables in the design matrix are calculated in Table 3. The relationship between coded and actual values is described by the following equation:

$$x = \frac{(x_i - x_0)}{\Delta x} \tag{3}$$

Table 3 | Factors and levels of BBD for the SSD

		Coded levels		
Variable	Factor	−1	0	1
N	X_1	23	25	27
N_F	X_2	10	12	14
D (%)	X_3	0.14	0.15	0.16
R	X_4	4	5.5	7

where x is the coded value, x_i is the actual value, x_0 is the actual value at the center point, and Δx is the step change value of the variables (Bezerra *et al.* 2008).

RESULTS AND DISCUSSION

Effect of NaOH addition on nitrogen removal rate

To determine the NaOH addition for the RD, some trials were done for the ratio of the actual value to theoretical value of NaOH in the range of 60%–120%. As shown in Figure 4, at the early stage of NaOH addition, the nitrogen content in the wastewater does not change significantly. When addition of NaOH reaches a certain value, the removal rate of nitrogen increases obviously. The possible reason is that ammonia is particularly soluble in water and inhibits the removal of ammonia when NH_4AC is not reacted completely. With the addition of NaOH, the increased hydroxide ions inhibit the dissolution of ammonia in water,

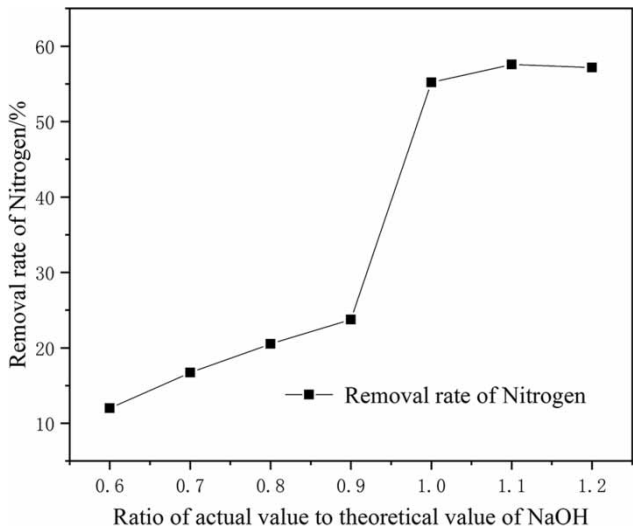

Figure 4 | Influence of addition amount of sodium hydroxide.

which is conducive to the removal of ammonia nitrogen. According to Figure 4 and Table 4, the optimal addition of NaOH was 7.12 g/100 g, the same as the theoretical value.

Effect of D_1 on SSD

The increase of D_1 is conducive to the collection of light components on the top of the tower. So it promotes the improvement of yield of methanol on the tower top (η_{CH_4O}) and the reduction of ω_{CH_4O-2}. However, when D_1 exceeds a certain range, it will accelerate the increase of tower temperature and disqualification of the top product. Therefore, it is necessary to investigate the effect of D_1 on SSD. D_1 was set as 0.11, 0.12, 0.13, 0.14, 0.15, 0.16, 0.17 and 0.18 respectively, when other conditions were N of 25, N_F of 12th, N_s of 24th, feeding quantity (F) of l00 kg/h, D_2 of 0.7 and R of 6.

As shown in Figure 5(a), at the beginning, η_{CH_4O} increases gradually while ω_{CH_4O-1} has no evident changes with the increase of D_1, and ω_{CH_4O-2} decreases gradually. When D_1 increases to 0.15, ω_{CH_4O-1} and η_{CH_4O} reach the maximum, and ω_{CH_4O-2} is at a low level. Therefore, D_1 was chosen to be 0.15.

Effect of R on SSD

The product purity on the top of the tower can improve with the increase of R. But too large R causes too much material circulation, and the tower balance will be broken. R was set as 1, 1.5, 2, 2.5, 3, 3.5, 4, 4.5, 5, 5.5, 6, 6.5 and 7 respectively, with N of 25, N_F of 12th, N_s of 24th, D_1 of 0.15 and D_2 of 0.45.

Table 4 | Influence of addition amount of sodium hydroxide

No.	Theoretical value of NaOH/g	Ratio of actual value to theoretical value of NaOH	Content of nitrogen after reaction/%	Quality of remaining liquid after reaction/g	Removal rate of nitrogen/ %
1	–	–	2.49	300.00	–
2	21.36	0.60	2.07	317.60	11.99
3	21.36	0.70	1.97	315.80	16.72
4	21.36	0.80	1.90	312.50	20.52
5	21.36	0.90	1.82	313.00	23.74
6	21.36	1.00	0.986	339.40	55.20
7	21.36	1.10	0.993	319.20	57.57
8	21.36	1.20	0.991	323.00	57.15

As shown in Figure 5(b), with the increase of R, ω_{CH_4O-1} and η_{CH_4O} increase, while ω_{CH_4O-2} decreases gradually. When R exceeds 6, ω_{CH_4O-1} is higher than 99% with ω_{CH_4O-2} lower than 0.1%, and the variation trends are not obvious. Therefore the appropriate R was selected as 6.

Effect of D_2 on SSD

Too large D_2 can reduce the heat transfer efficiency, affect the concentration of $(NH_4)_2SO_4$, and cause crystallization at the tower bottom. Therefore, it is necessary to investigate the influence of D_2.

As shown in Figure 5(c), with the increase of D_2, all three parameters decrease slowly within the fluctuation range allowed by the design. ω_{CH_4O-2} is lower than 0.1%, and subsequent biochemical treatment can be performed directly. Meanwhile, D_2 should be lower than 0.75 to avoid precipitation of $(NH_4)_2SO_4$ at the tower bottom. Moreover, in order to facilitate the subsequent recovery, the residue at the tower bottom should be a saturated solution of $(NH_4)_2SO_4$. Therefore, the selected D_2 was 0.7.

Effect of N on SSD

N was set as 15, 16, 17, 18, 19, 20, 21, 22, 23, 24, 25, 26, 27 and 28 respectively, when other conditions were fixed. As shown in Figure 5(d), with the increase of N, ω_{CH_4O-1} and η_{CH_4O} increase gradually, while ω_{CH_4O-2} decreases. When N exceeds 25, the growth rate of ω_{CH_4O-1} and η_{CH_4O} slow down gradually, while the decline rate of ω_{CH_4O-2} is gentle. Therefore, N of 25 was chosen in the later experiments.

Effect of N_F on SSD

The distillation efficiency will be affected when significant difference exists between the input concentration and the material concentration in the tower at the feeding port. For this purpose, the influence was studied at N_F of 3th, 4th, 5th, 6th, 7th, 8th, 9th, 10th, 11th, 12th, 13th, 14th and 15th, with other parameters fixed. The result is presented in Figure 5(e). With the increase of N_F, the separation of light components becomes more adequate, ω_{CH_4O-1} and η_{CH_4O} increase and ω_{CH_4O-2} decreases gradually. When N_F reaches 6th, the curves flatten out. As N_F reaches 12th, significant difference exists between the input concentration and the material concentration in the tower at the feeding position, which results in a decrease of distillation efficiency; ω_{CH_4O-1} and η_{CH_4O} decrease gradually. Considering

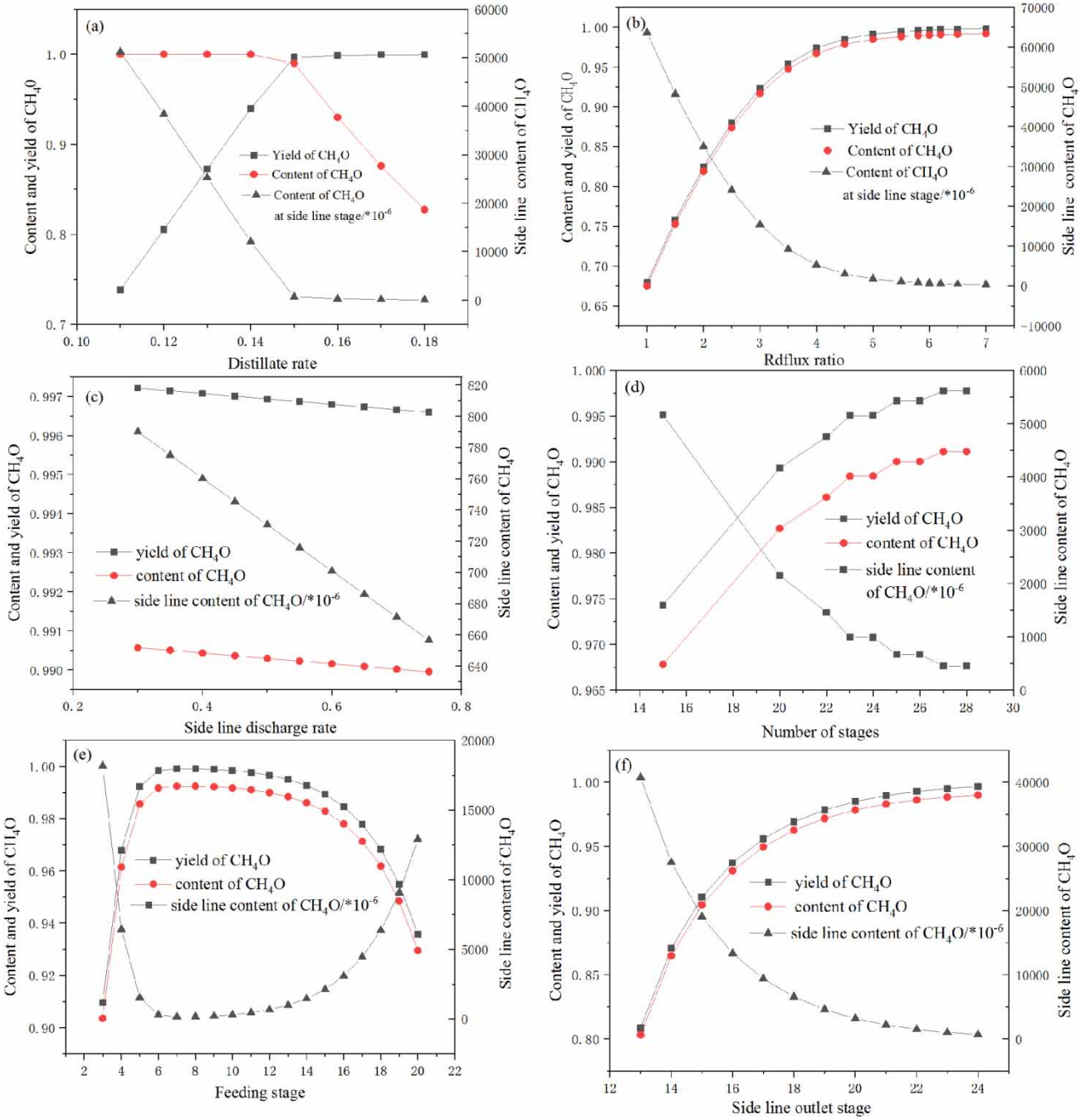

Figure 5 | Effect of (a) distillate rate (b) reflux ratio (c) side line discharge rate (d) number of stages (e) feed stage (f) side line outlet stage on side stream distillation.

the separation requirements and operating cost, 12th plate was selected as the proper N_F.

Effect of N_S on SSD

As shown in Figure 5(f), with the increase in N_S, ω_{CH_4O-1} and η_{CH_4O} increase and ω_{CH_4O-2} decreases gradually. When N_S reaches 24th, ω_{CH_4O-1} and η_{CH_4O} maximize, and ω_{CH_4O-2} reaches the minimum. Based on the above analysis, 24th stage was chosen as the appropriate N_S.

Box–Behnken design results and response surface analysis

Table 5 represents the range of factors along with the 29 tests designed. Accordingly, the test results were fitted to a

Table 5 | The BBD for three-level-four-factor RSM

	Coded values				Actual values				Response
Run	X_1	X_2	X_3	X_4	X_1	X_2	X_3	X_4	ω_{CH_4O-1}
1	0	−1	−1	0	25	10	0.14	5.5	0.999948
2	1	0	−1	0	27	12	0.14	5.5	0.999996
3	1	0	0	−1	27	12	0.15	4.0	0.975289
4	0	0	0	0	25	12	0.15	5.5	0.985383
5	0	0	1	1	25	12	0.16	7.0	0.930684
6	0	0	1	−1	25	12	0.16	4.0	0.921344
7	0	−1	0	1	25	10	0.15	7.0	0.992736
8	−1	−1	0	0	23	10	0.15	5.5	0.988001
9	−1	0	1	0	23	12	0.16	5.5	0.926662
10	−1	0	−1	0	23	12	0.14	5.5	0.999993
11	0	0	0	0	25	12	0.15	5.5	0.987065
12	0	−1	1	0	25	10	0.16	5.5	0.930431
13	0	1	1	0	25	14	0.16	5.5	0.926662
14	0	0	0	0	25	12	0.15	5.5	0.988374
15	0	0	0	0	25	12	0.15	5.5	0.989992
16	0	0	−1	−1	25	12	0.14	4.0	0.998922
17	−1	0	0	−1	23	12	0.15	4.0	0.956037
18	0	1	0	−1	25	14	0.15	4.0	0.956049
19	1	0	0	1	27	12	0.15	7.0	0.992749
20	−1	0	0	1	23	12	0.15	7.0	0.989679
21	1	−1	0	0	27	10	0.15	5.5	0.992065
22	0	0	−1	1	25	12	0.14	7.0	0.999998
23	1	1	0	0	27	14	0.15	5.5	0.988099
24	0	1	0	1	25	14	0.15	7.0	0.989687
25	−1	1	0	0	23	14	0.15	5.5	0.972879
26	0	0	0	0	25	12	0.15	5.5	0.983059
27	0	−1	0	−1	25	10	0.15	4.0	0.975108
28	0	1	−1	0	25	14	0.14	5.5	0.999999
29	1	0	1	0	27	12	0.16	5.5	0.930436

quadratic polynomial model to correlate the measured response with the independent factors. The analysis of variance (ANOVA) for the BBD is shown in Table 6. As can be seen, an F-value of 44.74 and *P*-value less than 0.0001 indicate that the model is significant. The value of correlation coefficient (R^2 values of 0.9781) is in reasonable agreement with the adjusted-R^2 value (0.9563). The high value of R^2 and non significance of lack of fit ($P > 0.05$) demonstrate that only 2.19% of the total variation can not be explained by the empirical model and the models have nice interpretation of the correlation between the responses and experiment conditions. Accordingly, the model can be dependably used.

The quadratic polynomial regression model was used to express the effects of independent variables on responses according to the following equation:

$$y = b_0 + \sum_{i=1}^{n} b_i x_i + \sum_{i=1}^{n} b_{ii} x_i^2 + \sum_{1 \le i < j}^{n} b_{ij} x_i x_j + \varepsilon \quad (4)$$

where y is the response, b_0 is the model constant, b_i, b_{ii} and b_{ij} are the coefficients, x_i and x_j are independent variables, n is the amount of variables, and ϵ is the error. The final regression model in terms of coded factors for ω_{CH_4O-1} is expressed by the following equation:

$$\begin{aligned}\omega_{CH_4O-1} = {} & 0.99 + 0.003782x_1 - 0.003743x_2 - 0.036x_3 \\ & + 0.009399x_4 + 0.002789x_1x_2 + 0.0009428x_1x_3 \\ & - 0.004046x_1x_4 - 0.0009552x_2x_3 + 0.004003x_2x_4 \\ & + 0.002066x_3x_4 - 0.001629x_1^2 - 0.001656x_2^2 \\ & - 0.02x_3^2 - 0.005829x_4^2 \end{aligned} \quad (5)$$

By default, the high levels of the factors are coded as positive sign and the low levels of the factors are coded as negative sign.

The response surfaces can be visualized as contours and/or 3D plots to constitute the variations in the response with respect to two variables, by keeping the other variable fixed (Ai *et al.* 2015). Figure 6 shows both contours and 3D surface response plots for ω_{CH_4O-1} as a function of (a) N vs D, (b) N vs R, (c) N_F vs D, and (d) D vs R, respectively. The central coordinate points among the utmost contour levels in each of the figures indicate the optimum value of corresponding parameters. Figure 6(a) and 6(c) indicate that ω_{CH_4O-1} increases gradually with the decrease of D_1 from 0.16 to 0.14, regardless of N and N_F at low or high level. The optimum ω_{CH_4O-1} region can be found at D_1 in the range of 0.145–0.155, N of 24–26, and N_F of 11th–13th, indicating that the effect of D_1 on ω_{CH_4O-1} is highly significant. Meanwhile, Figure 6(b) indicates that the maximum of ω_{CH_4O-1} is obtained at N of 25 and R of 5.5 with R having more effect than N. Figure 6(d) shows the effect of D_1 and R on ω_{CH_4O-1}. It is known that ω_{CH_4O-1} decreases steeply with decrease of R and increase of D_1. As the figure reveals, both D_1 and R play major role in SSD.

To further validate optimal values, the first partial derivative of regression equation was taken and made zero. It was concluded that the optimal values of the

Table 6 | ANOVA results for the response surface quadratic model

Source	SS	df	MS	F-Value	*P*-Value	
Model	0.020	14	1.420×10^{-3}	44.74	<0.0001	Significant
A-N	1.716×10^{-4}	1	1.716×10^{-4}	5.41	0.0356	
B-NF	1.681×10^{-4}	1	1.681×10^{-4}	5.30	0.0372	
C-D	0.016	1	0.016	491.58	<0.0001	
D-R	1.060×10^{-3}	1	1.060×10^{-3}	33.41	<0.0001	
AB	3.112×10^{-5}	1	3.112×10^{-5}	0.98	0.3388	
AC	3.555×10^{-6}	1	3.555×10^{-6}	0.11	0.7428	
AD	6.547×10^{-5}	1	6.547×10^{-5}	2.06	0.1728	
BC	3.649×10^{-6}	1	3.649×10^{-6}	0.12	0.7395	
BD	6.408×10^{-5}	1	6.408×10^{-5}	2.02	0.1772	
CD	1.707×10^{-5}	1	1.707×10^{-5}	0.54	0.4754	
A2	1.721×10^{-5}	1	1.721×10^{-5}	0.54	0.4736	
B2	1.780×10^{-5}	1	1.780×10^{-5}	0.56	0.4663	
C2	2.589×10^{-3}	1	2.589×10^{-3}	81.61	<0.0001	
D2	2.204×10^{-4}	1	2.204×10^{-4}	6.95	0.0196	
Residual	4.442×10^{-4}	14	3.173×10^{-5}			
Lack of Fit	4.155×10^{-4}	10	4.155×10^{-5}	5.78	0.0527	Not significant
Pure Error	2.874×10^{-5}	4	7.184×10^{-6}			
R^2	0.9781					
R^2_{adj}	0.9563					

Note: df, degree of freedom; MS, mean square; SS, sum of squares.
**P*-value <0.05 indicates statistical significance.

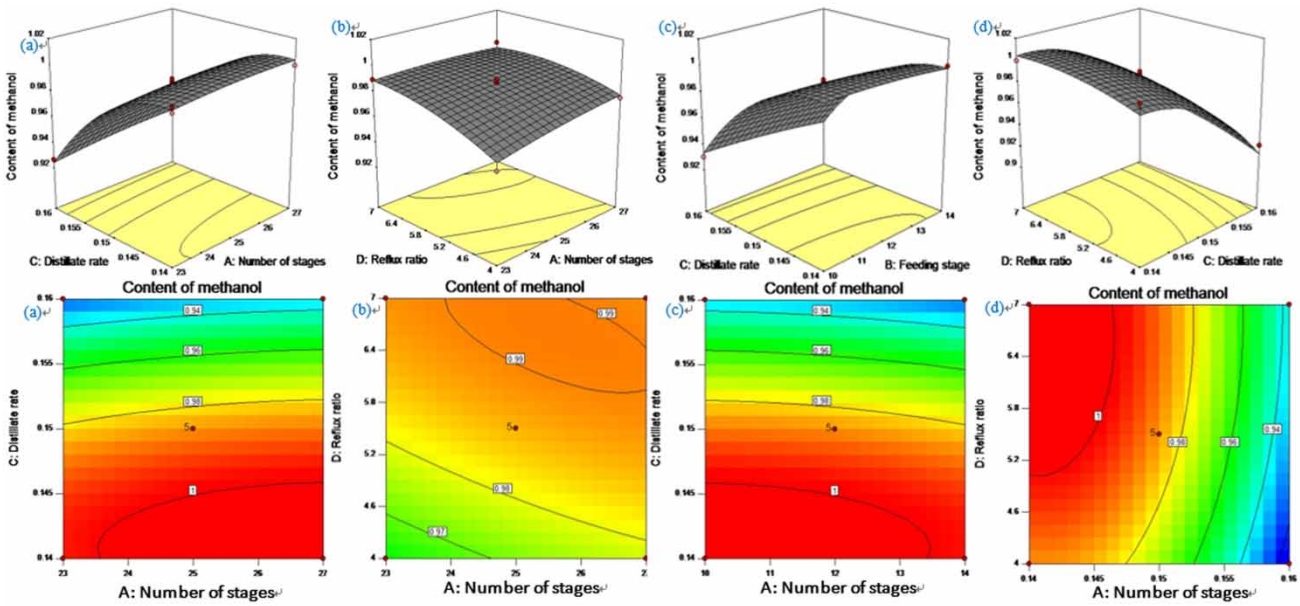

Figure 6 | Contours and 3D surface plots of the content of methanol for (a) number of stages vs. distillate rate, (b) number of stages vs. reflux ratio, (c) feeding stage vs. distillate rate, and (d) distillate rate vs. reflux ratio.

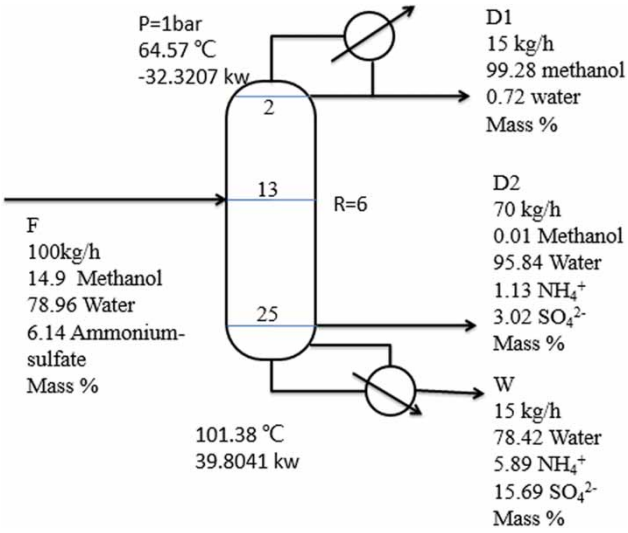

Figure 7 | Optimal flow sheet for SSD.

variables determined by RSM were N of 26, D of 0.15, R of 6 and N_F of 13th. In these conditions, the predicted value of ω_{CH_4O-1} was 99.5%. To check the validity of RSM, a verifying SSD experiment was conducted under the optimal condition and ω_{CH_4O-1} was 99.28%. The experimental value was close to the theoretical predicted value, indicating the practicability of optimizing the operating conditions of SSD by RSM method. Optimal flow sheet for SSD with equipment data, steam data, reflux ratio, heat duties and operating pressures (P) is shown in Figure 7.

PRACTICAL APPLICATIONS AND FUTURE RESEARCH PERSPECTIVES

There has been very little research on pymetrozine production wastewater treatment. In terms of this issue, a pretreatment solution was provided to effectively remove nitrogen and purify methanol. The follow-up work is organic nitrogen compounds removal by complex extraction and advanced treatment of the extracted aqueous phase in order to reduce harmful substances and meet the direct emission standards. This method can also be used for pretreatment of other pesticide production wastewater and simplify the subsequent treatment process.

CONCLUSIONS

In the present work, ammonia conversion treatment and SSD process were conducted to pretreat the pymetrozine production wastewater. Aspen Plus software was used to simulate the single factor experiment of SSD. BBD based on RSM was employed to evaluate the optimal operational conditions, and D_1 and R were chosen as the most significant factor. A verifying experiment was conducted to check the validity of RSM. Optimum separation result was obtained as ω_{CH_4O-1} of 99.28% with η_{CH_4O} of 99.95%, ω_{CH_4O-2} less than 0.1%, and $(NH_4)_2SO_4$ content of 21.58% at the tower bottom, at N of 26, D_1 of 0.15, R of 6 and N_F of 13th.

ACKNOWLEDGEMENT

This work was supported by Extraction Engineering Technological Research Center of Jiangsu province and Key Laboratory of Integrated Regulation and Resource Development on Shallow Lake of Ministry of Education.

This work was sponsored by National Natural Science Foundation of China (Grant No. 51979077), the Fundamental Research Funds for the Central Universities (Grant No. 2019B42414) and Jiangsu Provincial Science and Technology Program Project (Grant No. SBA2018030430 and BE2019121).

DATA AVAILABILITY STATEMENT

All relevant data are included in the paper or its Supplementary Information.

REFERENCES

Ai, C., Zhou, D., Wang, Q., Shao, X. & Lei, Y. 2015 Optimization of operating parameters for photocatalytic degradation of tetracycline using In2S3 under natural solar radiation. *Solar Energy* **113**, 34–42.

Bezerra, M. A., Santelli, R. E., Oliveira, E. P., Villar, L. S. & Escaleira, L. A. 2008 Response surface methodology (RSM) as a tool for optimization in analytical chemistry. *Talanta* **76** (5), 965–977.

Carra, I., Sánchez Pérez, J. A., Malato, S., Autin, O., Jefferson, B. & Jarvis, P. 2016 Performance of different advanced oxidation processes for tertiary wastewater treatment to remove the pesticide acetamiprid. *Journal of Chemical Technology & Biotechnology* **91** (1), 72–81.

Cordova-Villegas, L. G., Cordova-Villegas, A. Y., Taylor, K. E. & Biswas, N. 2019 Response surface methodology for optimization of enzyme-catalyzed azo dye decolorization. *Journal of Environmental Engineering* **145** (5), 04019013.

De Gaetano, Y., Hubert, J., Mohamadou, A., Boudesocque, S., Plantier-Royon, R., Renault, J.-H. & Dupont, L. 2016 Removal of pesticides from wastewater by ion pair centrifugal partition extraction using betaine-derived ionic liquids as extractants. *Chemical Engineering Journal* **285**, 596–604.

Elfikrie, N., Ho, Y. B., Zaidon, S. Z., Juahir, H. & Tan, E. S. S. 2020 Occurrence of pesticides in surface water, pesticides removal efficiency in drinking water treatment plant and potential health risk to consumers in Tengi River Basin, Malaysia. *Science of The Total Environment* **712**, 136540.

Fdez-Sanromán, A., Acevedo-García, V., Pazos, M., Sanromán, M. Á. & Rosales, E. 2020 Iron-doped cathodes for electro-Fenton implementation: application for pymetrozine degradation. *Electrochimica Acta* **338**, 135768.

Gor, N. K., Mali, N. A. & Joshi, S. S. 2020 Intensified reactive distillation configurations for production of dimethyl ether. *Chemical Engineering and Processing – Process Intensification* **149**, 107824.

Hou, J., Xie, W., Hong, D., Zhang, W., Li, F., Qian, Y. & Han, C. 2019 Simultaneous determination of ten neonicotinoid insecticides and two metabolites in honey and royal-jelly by solid-phase extraction and liquid chromatography-tandem mass spectrometry. *Food Chemistry* **270**, 204–213.

Jang, J., Rahman, M. M., Ko, A. Y., Abd El-Aty, A. M., Park, J. H., Cho, S. K. & Shim, J. H. 2014 A matrix sensitive gas chromatography method for the analysis of pymetrozine in red pepper: application to dissipation pattern and PHRL. *Food Chemistry* **146**, 448–454.

Kahoush, M., Behary, N., Cayla, A. & Nierstrasz, V. 2018 Bio-Fenton and Bio-electro-Fenton as sustainable methods for degrading organic pollutants in wastewater. *Process Biochemistry* **64**, 237–247.

Karthikeyan, K., Nanthakumar, K., Shanthi, K. & Lakshmanaperumalsamy, P. 2010 Response surface methodology for optimization of culture conditions for dye decolorization by a fungus, *Aspergillus niger* HM11 isolated from dye affected soil. *Iranian Journal of Microbiology* **2** (4), 213.

Khan, I., Bano, M., Khan, G. A. & Khan, F. 2018 Design of functionalized-ZnNP decorated fMWCNT-IL composite CPE: an ideal electrode material for enhanced electrocatalytic determination of pymetrozine. *Materials Science and Engineering: B* **238–239**, 83–92.

Olfati Somar, R., Zamani, A. A. & Alizadeh, M. 2019 Joint action toxicity of imidacloprid and pymetrozine on the melon aphid, *Aphis gossypii*. *Crop Protection* **124**, 104850.

Qin, H., Guo, W., Huang, X., Gao, P. & Xiao, H. 2020 Preparation of yttria-stabilized ZrO_2 nanofiltration membrane by reverse micelles-mediated sol-gel process and its application in pesticide wastewater treatment. *Journal of the European Ceramic Society* **40** (1), 145–154.

Rajapaksha, P. P., Power, A., Chandra, S. & Chapman, J. 2018 Graphene, electrospun membranes and granular activated carbon for eliminating heavy metals, pesticides and bacteria in water and wastewater treatment processes. *Analyst* **143** (23), 5629–5645.

Sutton, R., Xie, Y., Moran, K. D. & Teerlink, J. 2019 Occurrence and sources of pesticides to urban wastewater and the environment. In: *Pesticides in Surface Water: Monitoring, Modeling, Risk Assessment, and Management*. ACS Publications, pp. 63–88.

Tony, M. A. & Mansour, S. A. 2019 Microwave-assisted catalytic oxidation of methomyl pesticide by $Cu/Cu_2O/CuO$ hybrid nanoparticles as a Fenton-like source. *International Journal of Environmental Science and Technology* **17** (1), 161–174.

Tututi-Avila, S., Medina-Herrera, N., Hahn, J. & Jiménez-Gutiérrez, A. 2017 Design of an energy-efficient side-stream extractive distillation system. *Computers & Chemical Engineering* **102**, 17–25.

Wang, B., Ke, S., Kishore, B., Xu, X., Zou, Z. & Li, Z. 2012 A facile synthesis of pyrimidone derivatives and single-crystal characterization of pymetrozine. *Synthetic Communications* **42** (16), 2327–2336.

Wang, K., Cai, Q., Gu, Z., Sun, H. & Huang, X. 2020 Optimization of organic nitrogen compounds removal in pymetrozine production wastewater using complex extraction with response-surface methodology. *Journal of Environmental Engineering* **146** (7), 04020068.

Wei, X., Xu, X., Yang, X., Li, J. & Liu, Z. 2020 Visible light degradation of reactive black-42 by novel $Sr/Ag\text{-}TiO_2$@g-C_3N_4 photocatalyst: RSM optimization, reaction kinetics and pathways. *Spectrochim Acta A Mol Biomol Spectrosc* **228**, 117870.

Zhou, Q., Du, F., Shi, Y., Liu, W., Liu, D. & Chen, G. 2018 An efficient protocol for the production of pymetrozine via a new synthetic strategy. *Journal of Chemical Research* **42** (8), 434–438.

First received 14 September 2020; accepted in revised form 7 December 2020. Available online 18 December 2020